Climate Dynamics (2019) 52:69–82
https://doi.org/10.1007/s00382-018-4138-y

How autumn Eurasian snow anomalies affect east asian winter monsoon: a numerical study

Xiao Luo[1] · **Bin Wang**[1,2]

Received: 6 June 2017 / Accepted: 3 January 2018 / Published online: 5 March 2018

Abstract
Previous studies have found that snow Eurasian anomalies in autumn can affect East Asian winter monsoon (EAWM), but the mechanisms remain controversial and not well understood. The possible mechanisms by which Eurasian autumn snow anomalies affect EAWM are investigated by numerical experiments with a coupled general circulation model and its atmospheric general circulation model component. The leading empirical orthogonal function mode of the October–November mean Eurasian snow cover is characterized by a uniform anomaly over a broad region of central Eurasia (40°N–65°N, 60°E–140°E). However, the results from a 150-ensemble mean simulation with snow depth anomaly specified in October and November reveal that the Mongolian Plateau and Vicinity (MPV, 40°–55°N, 80°–120°E) is the key region for autumn snow anomalies to affect EAWM. The excessive snow forcing can significantly enhance EAWM and the snowfall over the northwestern China and along the EAWM front zone stretching from the southeast China to Japan. The physical process involves a snow-monsoon feedback mechanism. The excessive autumn snow anomalies over the MPV region can persist into the following winter, and significantly enhance winter snow anomalies, which increase surface albedo, reduce incoming solar radiation and cool the boundary layer air, leading to an enhanced Mongolian High and a deepened East Asian trough. The latter, in turn, strengthen surface northwesterly winds, cooling East Asia and increasing snow accumulation over the MPV region and the southeastern China. The increased snow covers feedback to EAWM system through changing albedo, extending its influence southeastward. It is also found that the atmosphere–ocean coupling process can amplify the delayed influence of Eurasian snow mass anomaly on EAWM. The autumn surface albedo anomalies, however, do not have a lasting "memory" effect. Only if the albedo anomalies are artificially extended into December and January, will the EAWM be affected in a similar way as the impacts of autumn snow mass anomalies.

Keywords Snow-monsoon feedback mechanism · East Asian winter monsoon · Eurasian snow cover · Surface albedo · Coupled climate model

1 Introduction

Strong East Asian winter monsoon (EAWM) often brings cold surges and blizzard to Asian countries, resulting in heavy economic losses. The year-to-year variation of the EAWM is therefore among the utmost issues of climate prediction (Wang and Lu 2016).

Snow is an important component of the hydroclimate system. Variations of snow cover can modulate radiative, moisture and heat exchanges between the atmosphere and land surface. Physically, snow cover and snow depth could affect the atmospheric circulation through altering surface albedo and soil moisture during the melting process (Hahn and Shukla 1976; Barnett et al. 1989). Therefore, the interaction between snow cover/snow depth anomalies in local and remote atmospheric dynamics has been an interesting subject of research.

The impacts of snow cover/snow depth over Eurasian continent have been widely studied with respect to its close relationship with the active Asian monsoon activity, which

✉ Bin Wang
wangbin@hawaii.edu

[1] Department of Atmospheric Sciences and Atmosphere-Ocean Research Center, University of Hawaii at Manoa, Honolulu, HI 96822, USA

[2] Earth System Modeling Center, Nanjing University of Information Science and Technology, Nanjing 210044, China

includes spring snow effect on summer monsoon and fall snow impact on winter monsoon. For the spring snow anomalies, an inverse relationship between Indian Summer monsoon rainfall and Eurasian spring snowfall was noticed (Hahn and Shukla 1976). Yim et al. (2010) further found two distinct patterns of spring Eurasian snow cover anomaly which could have different impacts on East Asia summer monsoon. The autumn snow anomalies can also influence the subsequent winter atmospheric circulation. Some observational studies pointed out excessive autumn snow over the Eurasian continent can decrease the surface temperature and foreshadow a bitter winter with strong winter monsoon (Jhun and Lee 2004; Wang et al. 2010). Watanabe and Nitta (1998a) showed that a decrease of snow cover over East Asia (EA) in autumn can lead to an increase in surface temperature in East Asia, and a decrease in sea level pressure and geopotential height at 500 hPa in the Arctic region. Cohen and Entekhabi (1999) found that Eurasian snow cover extent in October correlates well with the Northern Annular Mode pattern in the following January. Wang et al. (2009) suggested the decrease of snow depth over the Eurasian continent and North America around 1988 plays an important role in the decadal weakening of wavenumber 2, and further weakens EAWM.

Varieties of precursors for seasonal prediction of EAWM have been documented, including developing El Niño/Southern Oscillation (ENSO) events (Zhang et al. 1996; Wang et al. 2000), Arctic sea ice concentration anomalies (Honda et al. 2009; Wu et al. 2011) and Eurasian snow cover anomalies in the preceding autumn (Clark and Serreze 2000; Watanabe and Nitta 1998a). Wang et al. (2010) revealed two dominant modes of the EAWM; the cold northern mode is preceded by excessive snow covers over southern Siberia–Mongolia, while the cold southern mode is preceded by development of La Nina episodes and reduced snow covers over the northeast Siberia. Among these slow varying anomalous lower boundary precursors, the autumn snow cover and snow depth anomaly were found to be an important source of variability, especially for the higher latitude Eurasian regions where El Niño/Southern Oscillation (ENSO) has a relatively small impact (Watanabe and Nitta 1998b; Cohen and Fletcher 2007).

Several mechanisms have been proposed to explain the linkage between autumn snow anomaly and winter circulation anomalies. Watanabe and Nita (1998b) conducted a light snow numerical experiment using an atmospheric general circulation model (AGCM) which employed observed Eurasian negative snow anomalies from September to the following February in 1988/1999 as boundary forcing. They found the surface warming over Eurasia in 1989 winter is reproduced through a local energy balance associated with reduced albedo and net shortwave radiation. They also suggested that the simulated wintertime dipole anomalies with positive in midlatitudes and negative in polar regions could be the key atmospheric responses at 500 hPa to snow forcing, and thus large scale thermal advection also influences temperature over Eurasia. Furthermore, Jhun and Lee (2004), based on their AGCM numerical experiment result, indicated that the decrease of snow in autumn over East Asia could stimulate surface warming and upward motion, and induce a compensating descent over the North Pacific, which weakens the Aleutian low and EAWM. More recently, from a wave propagation perspective, Cohen et al. (2007) pointed out that Eurasian snow cover extent in October are linked with the Northern Annular mode or Arctic Oscillation (AO) in the following January through a dynamical process that includes anomalous vertical propagation of Rossby wave activity. They proposed a dynamical pathway mechanism: Snow cover increases rapidly over Siberia in fall; the associated diabatic cooling can then reinforce the Siberian high and decrease surface temperature; the snow forced diabatic cooling can increase the upward propagation of stationary waves in the troposphere; the absorption of wave in stratosphere in late fall and early winter will lead to weakened polar vortex and a warming downward from the stratosphere to the surface several weeks later. When the hemispheric signal reaches the surface, it will project onto a negative Arctic Oscillation (AO) pattern. Although some modeling experiments with prescribed observed snow cover can reproduce the above statistical relationship (Gong et al. 2003; Fletcher et al. 2009; Peings et al. 2012), recent studies have pointed out that the current dynamical models could not recover Eurasian snow cover-AO relationship when snow cover is internally generated rather than artificially specified (Hardiman et al. 2008; Furtado et al. 2015). Therefore, it remains under debate concerning the physical processes by which autumn Eurasian snow anomalies affect winter climate. We will investigate this issue using both coupled and atmospheric dynamical models.

In this study, we intend to reexamine the mechanisms by which autumn snow anomalies affect winter temperature and precipitation using a state-of-the-art dynamical model. We design two types of experiments, i.e., prescribe snow depth and surface albedo anomalies in the previous autumn to examine the following issues: (1) what is the lead-lag relationship between Eurasian snow anomaly and the subsequent winter circulation? And (2) what are the physical processes captured by the current AGCM and coupled general circulation model (CGCM)? In addition, since snow could modulate surface heat flux mainly through changing surface albedo, we also wonder whether an artificial surface albedo anomaly in autumn can persist into winter.

Section 2 introduces the model we used and the design of numerical experiments. In Sect. 3, we identify the snow mass forcing region over Eurasian continent. Section 4 presents the results from numerical experiments associated with

anomalous autumn snow depth and illustrates the physical mechanism by which autumn snow anomalies affect EAWM. Section 5 further shows the results from additional sensitivity numerical experiments with regard to the location of the forcing as well as an albedo perturbation. Summary and discussion are provided in Sect. 6.

2 Data and numerical experiments

2.1 Data

The observed weekly snow cover extent data are obtained from the Rutgers Global Snow Laboratory (Robinson et al. 1993), which cover the period of 1973–2013. The data prior to June 1999 are based on weekly satellite-derived snow cover extent maps, and the data after that are derived from the daily Interactive Multisensor Snow and Ice Mapping System high resolution (88 × 88 cell) product. The snow cover extent data have been used in international assessments of climate variability and change (Robinson et al. 2012).

2.2 Numerical model

The coupled model used is the Nanjing University of Information Science and Technology coupled Earth System Model (NUIST-ESM) v1a (Cao et al. 2015). This NUIST-ESM consists of an atmospheric component using the European Centre Hamburg Model version 5.3 (ECHAM5.3), an oceanic component using version 3.4 of the Nucleus for European Modeling of the Ocean (NEMO), and a sea ice component using version 4.1 of the Los Alamos sea ice model (CICE). The ECHAM 5.3 has a horizontal resolution of T42 spectral truncation (about 2.8° by 2.8°) and 31 vertical levels, and a detailed description could be found in Roeckner et al. (2003). The ocean model has 31 layers, and its horizontal resolution is 2° × 2°, with an increased resolution of 1/3° in the meridional direction in the equatorial region. ECHAM 5.3's simulation captures the interannual variability of snow cover area reasonably well (Roesch and Roeckner 2006). The NUIST-ESM has been used to study the atmosphere–ocean interaction processes that impact Indian summer monsoon rainfall and winter monsoon variability (Li et al. 2016; Luo and Wang 2017).

To demonstrate the fidelity of the NUIST-ESM for study of EAWM variability, the model simulated winter climatology from the control experiment is shown in Fig. 1. Overall, the model simulates realistic climatology of EAWM, including major circulation systems such as the Mongolian–Siberian High (MSH) over the mid-high latitude Eurasian continent and the Aleutian Low (AL) over the North Pacific Ocean (Fig. 1a, b), the northeast-southwest titled East Asian trough at 500 hPa level (Fig. 1c, d), and the subtropical jet and polar front jet over East Asia at 200 hPa level (Fig. 1c, d), as well as the 2 m air temperature (Fig. 1e, f). The positions of these main circulation components are well captured by model's simulation. The simulated intensity of the SH is in a better agreement with observations than the intensity of simulated AL and East Asian subtropical jet, which are slightly underestimated.

2.3 Experimental design

2.3.1 Specification of snow depth and snow cover anomalies

For snow depth experiment, we specify initial perturbations on the water equivalent snow depth because it is a useful diagnostic parameter in the model integration. Specifically, in ECHAM5.3, the SWE could be converted to snow cover fraction/extent (SCF) on the ground, which is crucial for computation of winter surface albedo (Roesch and Roeckner 2006). The SCF is diagnostically derived from SWE based on the following approximate equation:

$$\mathrm{SCF} = 0.95 \tanh(100SWE)\left(\frac{1000SWE}{1000SWE + \varepsilon + 0.15\sigma_Z}\right) \quad (1)$$

where σ_Z reflects the slope of the terrain, ε is a small number used to avoid division by zero on the flat grid cells without snow covering. A correct simulation of the SCF is crucial for the computation of surface albedo during the winter season (Roesch and Roeckner 2006).

2.3.2 Control and sensitivity experiments

1. Control run: to obtain atmospheric climatology in the model, ECHAM5.3 is integrated as a control run with prescribed climatological values of SST and sea ice concentration. Meanwhile, control run is also conducted for coupled model NUIST-ESM with a sample size of 150 years, which follows a spin-up for over 2000 years to reach an equilibrium state.
2. Water equivalent snow depth sensitivity experiment (SD experiment): To identify how the autumn snow mass impact the ensuing winter climate, we perform SD experiments with a water equivalent snow depth anomaly of 2.6 mm/day (or 8 cm/month) gradually added to the model snow depth field over the central Eurasian region (40°N–65°N, 60°E–140°E) starting from October 1 to November 30, and after November 30 the model runs without snow depth perturbation. The selection of the snow mass forcing region will be discussed in Sect. 2. Additional sensitivity tests are also performed with different regions and different amplitudes of snow

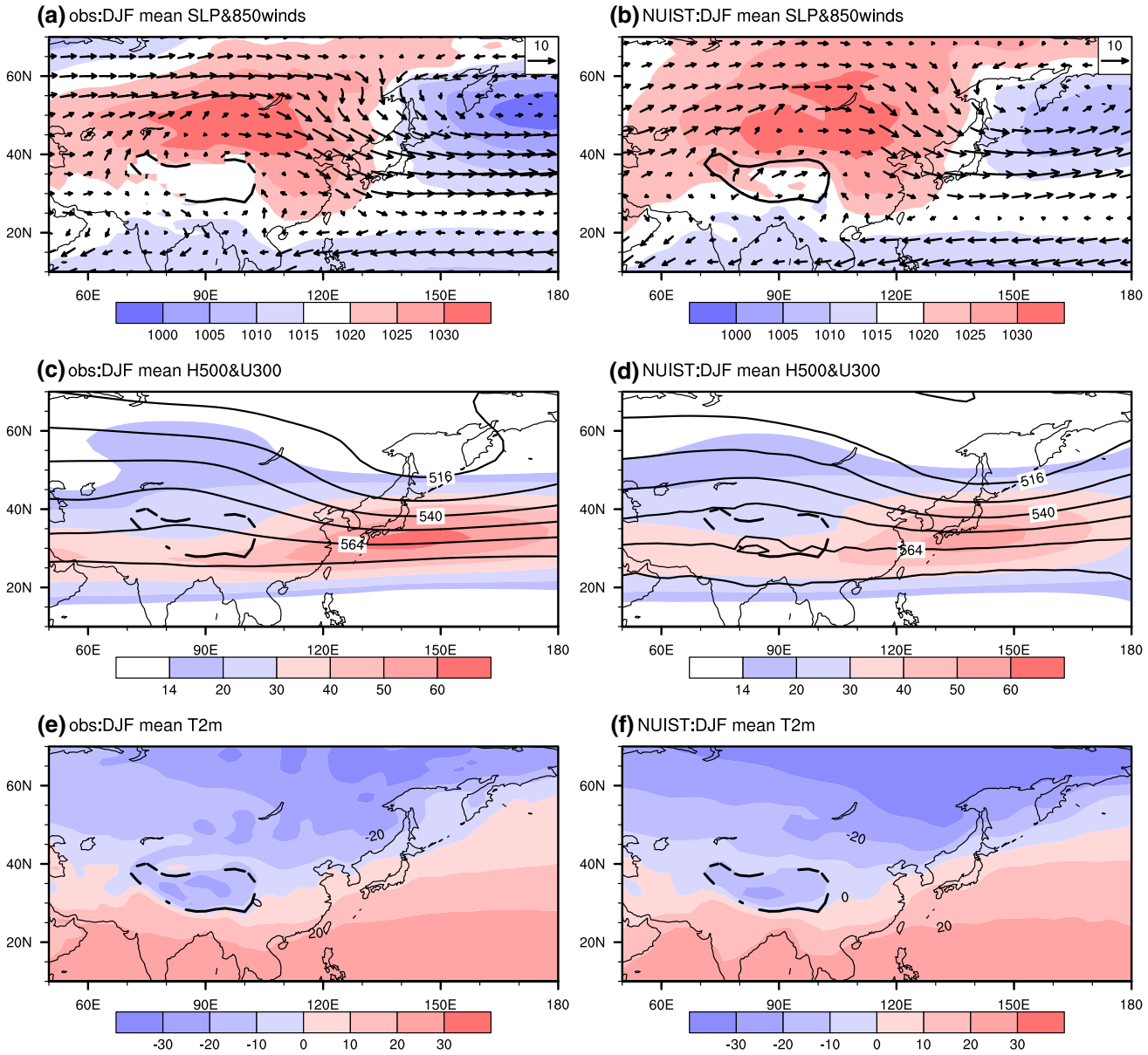

Fig. 1 Winter (DJF) mean circulations in the domain of Asian winter monsoon from observation (left panel) and simulated by NUIST-ESM (right panel). **a, b** Sea-level pressure (SLP; shaded; hPa) and 850 hPa winds (vectors; m s^{-1}), **c, d** 500 hPa geopotential height (contours; 10 gpm) and 300 hPa zonal wind (shaded; m s^{-1}), **e, f** 2 m air temperature. The 3000 m topographic contour outlines the location of the Tibetan Plateau

depth anomaly specified, and the results are discussed in Sect. 6.

Each set of the above experiments is performed using ECHAM5.3 and coupled model from NUIST respectively, and these parallel experiment results are used for comparing the differences between the AGCM and CGCM and assessing the role of atmosphere–ocean interaction.

2.3.3 Generation of ensemble results

Because of large internal variability in the mid-high latitudes, the ensemble size is set to 30 for the AGCM experiments and 150 for the CGCM experiments. Meanwhile, the t-test was used to determine the statistical significance of all the composites derived from the ensemble means.

3 The observed snow cover variability over Eurasian continent

Before conducting numerical experiments, we first take a look at the variability of snow cover extent in October and November over Eurasia. To identify the dominant variability patterns of Eurasian snow cover, we conducted Empirical Orthogonal Function (EOF) analysis on the October–November mean snow cover anomaly from 1973 to 2013 in the domain of 0°N–90°N, 20°E–150°E. Before conducting EOF analysis, the covariance matrix field is weighted using $\cos(\varphi)$, and φ refers to latitude.

The first three EOF modes account for 24.9, 14.1 and 10.7% of the total variance of latitudinal-weighted October–November mean snow cover extent. The leading EOF is significantly separated from the next two EOFs according to the criterion of North et al. (1982). The second and third EOFs are inseparable and have substantially lower contribution to the total variance. The spatial pattern of EOF1 is characterized by a continental scale of excessive (suppressed) snow cover anomaly covering the domain of 40°N–65°N, 60°E–140°E (Fig. 2a). The corresponding principal component (PC) exhibits notable interdecadal variations with reduced snow cover extent from the early 1980s to late 1990s (Fig. 2b) during a warm period of EAWM (Wang and Chen 2013). The period with excessive snow cover before the 1980s also corresponds to strong EAWM. This implies that as a dominant variability mode, EOF1 is closely linked to the ensuing winter Asian surface temperature. Therefore, in the following snow depth experiment, we select the domain of 40°N–65°N, 60°E–140°E as the snow mass forcing region. This domain is also consistent with the key Eurasian snow cover region based on observation suggested by Luo and Wang (2017), except the western boundary shifts 20° eastward, which is because the present study deals with the variation of snow cover in both October and November.

4 Impacts of central Eurasian snow mass anomaly on winter monsoon

In the SD experiment, a fundamental question is: Will the perturbed snow depth anomalies in October and November persist into winter? Furthermore, how do snow melting, evaporation and accumulation processes determine the persistence of snow mass over the Eurasian continent from October to the ensuing winter in the coupled model? Our analysis starts with addressing these questions.

4.1 Evolution of snow anomalies from autumn to winter

4.1.1 Water equivalent snow depth

Figure 3 shows the evolution of the spatial patterns of the monthly snow depth anomaly derived from the differences between the sensitivity experiments and the control run. The snow anomalies are gradually accumulated from October to November, and by the end of October, the anomalous water equivalent snow depth is above 6 cm to the north of 50°N over the specified forcing region. On the other hand, the snow mass in the southern part of the forcing region has much less accumulation due to snow melting at the lower latitudes (Fig. 3a). By the end of November, the anomalous water equivalent snow depth spatial pattern maintains the "more in the higher latitude and less in the lower latitude" pattern, except that a large quantity of over 15 cm is seen at the anomaly center (Fig. 3b). The anomalous snow

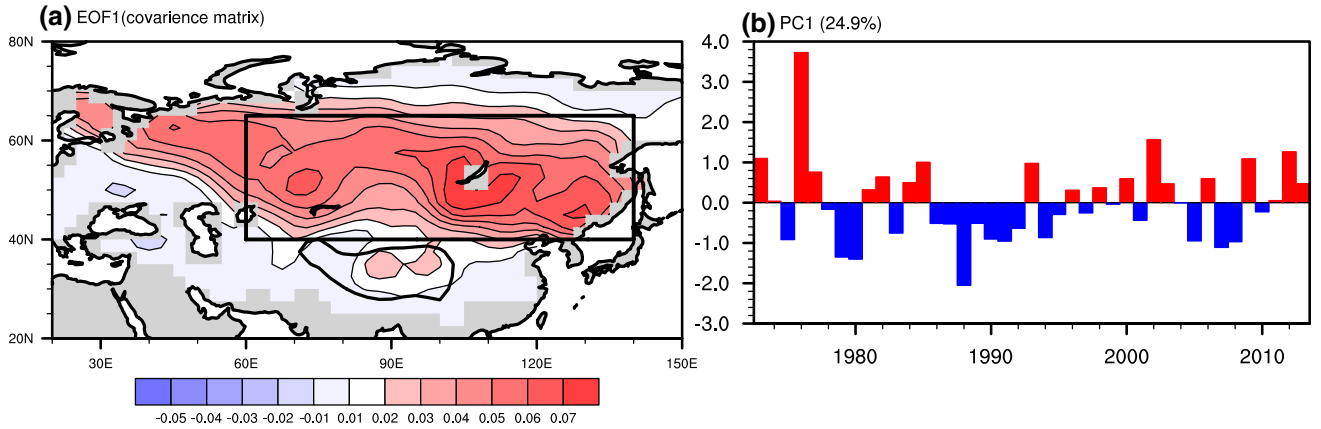

Fig. 2 Spatial pattern (**a**) and time series (**b**) of the leading mode of the October and November mean Snow cover extent derived by EOF analysis on latitudinal-weighted covariance matrix field. The thick black line is the 3000 m height contour, outlining the Tibetan Plateau. The black rectangular denotes the forcing region of snow cover extent anomaly

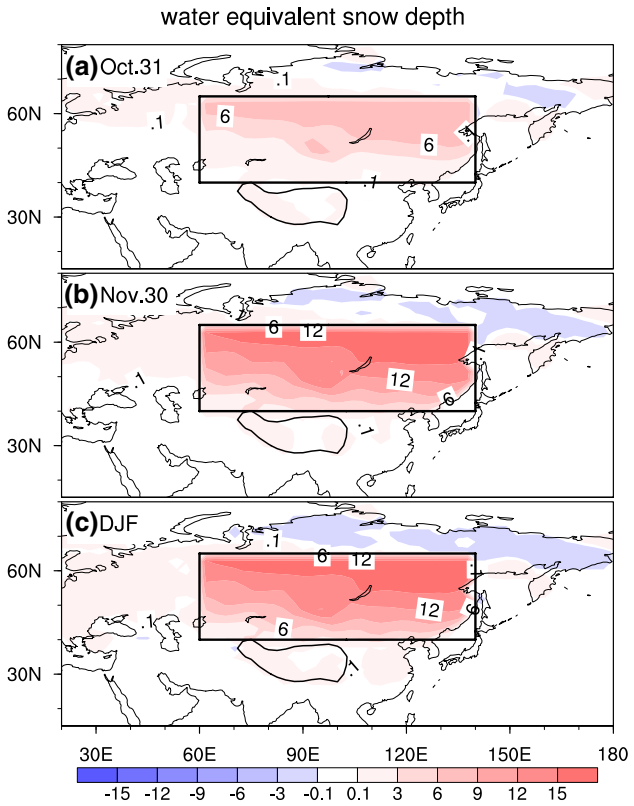

Fig. 3 Composite differences (SD experiment minus control run) of water equivalent snow depth (cm) on **a** November 30, **b** December 31 and **c** winter mean from the coupled model experiments

accumulation pattern during winter when the added snow depth anomalies had been switched off shows a pattern similar to that on November 30. Meanwhile, it is of interest to note that the positive snow depth anomalies extend a little bit southward in the following winter (Fig. 3c), especially over the central-eastern China.

4.1.2 Snow cover extent and surface albedo

Figure 4 presents the temporal evolution of snow cover fraction averaged over the Mongolian Plateau and Vicinity (MPV, 40°–55°N, 80°–120°E) region, which, as will be shown in Sect. 5.1, is a key region for autumn snow anomalies to affect EAWM. The snow cover fraction is derived from Eq. (1). In the control run, the snow cover increases gradually from October to February. On the other hand, in the sensitivity experiment, snow cover fraction increases rapidly from October to November as we specify excessive water equivalent snow depth during this period. The specified snow mass anomaly in the autumn gradually accumulates and is subject to slightly melting and evaporation. After December 1, the areal mean snow cover fraction maintains at 0.75 in winter, and starts to decrease in early March in the

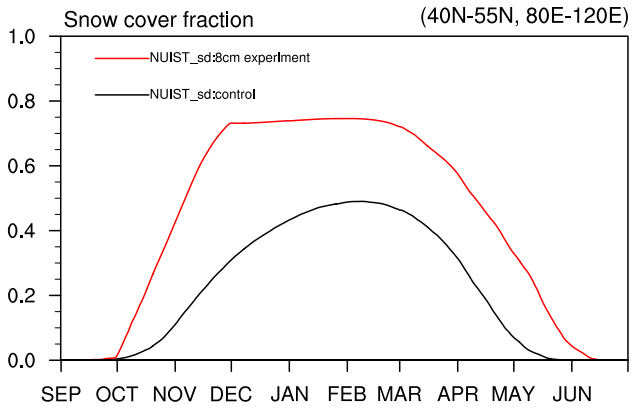

Fig. 4 Time series of snow cover fraction averaged over (40°–55°N, 80°–120°E) in coupled model SD numerical experiments. Red (black) lines are results from the 8 cm SD sensitivity numerical run (control run) experiments. Coupled model SD experiment's ensemble size is 150

SD experiment, which is delayed by about 2 weeks comparing with climatology in the control run.

Figure 5 presents the spatial patterns of snow cover fraction evolution from December to the following February. In the control run, the climatological snow cover occupies the Eurasian continent to the north of 50°N (Fig. 5a, c, e). In the SD sensitivity experiment, the anomalous snow cover fraction is significantly enhanced in the mid-latitude Eurasia, and the maximum increase is located in the latitude belt between 40°N and 50°N (Fig. 5b, d, f). Note that the increased winter snow cover extent is generally located at the southern part of snow perturbation domain. This is because climatologically, the high-latitude (north of 50°N) Eurasian continent is already covered by snow during winter; thus, an increase in snow depth could only slightly modulate the snow cover extent. In contrast, over the mid-latitude Eurasian region, especially over the mountain regions of the Mongolian Plateau and vicinity where it is less covered by snow in winter, the snow cover tends to increase much more significantly given an equal amount of the snow mass anomaly. It is also notable that the snow cover extent anomaly extends further southward to 30°N over East Asia during winter, especially in January and February (Fig. 5d, f). This southward expansion of snow cover fraction can also induce increased surface albedo over the eastern China, as will be shown in Fig. 6.

How does snow cover anomaly affect surface albedo? Figure 6 shows spatial patterns of anomalous surface albedo evolution from November to February. In November, the surface albedo is increased along the latitude belt between 45°N and 55°N, in particular over the Eastern Mongolia and Inner-Mongolia with the positive anomaly center exceeding 0.3 (Fig. 6a). During December, the belt of increased surface albedo shifts further southward by about 5° of latitude to

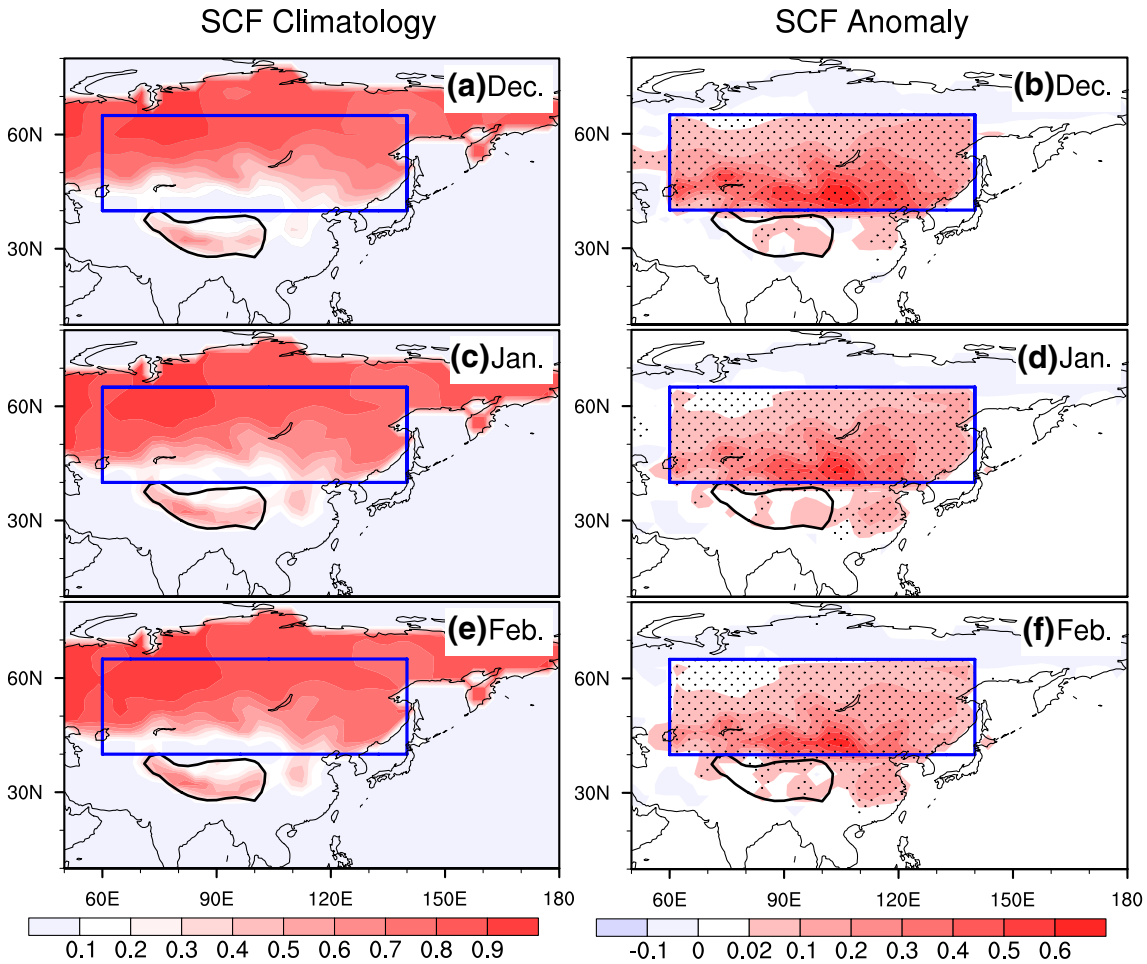

Fig. 5 Snow cover fraction in December (**a, b**), January (**c, d**) and February (**e, f**). Left panels (**a, c, e**) are climatology, and right panels (**b, d, f**) are composite differences (SD experiment minus control run) of snow cover fraction from the coupled model experiments. Dots in **b, d, f** indicate the anomalies of snow cover fraction significant at the 95% confidence level. The thick black line is the 3000 m height contour, outlining the Tibetan Plateau. The thick navy blue line outlines the boundary of China and Mongolia. The blue rectangular denotes the snow forcing region

northern China and maintains there in January and February (Fig. 6b–d). Also, the increased surface albedo extends further southward to 30°N in the central eastern China during January and February (Fig. 6c, d), corresponding to the southward expansion of snow cover extent anomaly (Fig. 5d, f). The evolution and persistence of surface albedo anomalies from October to December verify that the albedo change is closely linked to the snow cover extent anomaly over Eurasia, because it is the snow cover extent that modules surface albedo directly.

To see why the snow cover anomaly expands southward to the central eastern China in winter, we then examine the monthly snowfall anomaly (Fig. 7). In winter, the excessive snowfall occurs to the south and along the T2m 0 °C as shown by the blue lines in Fig. 7, primarily located along the EAWM front zone stretching from the southeast China to Japan (Fig. 7b–d). The anomalous snowfall over central eastern China is further enhanced in December and January (Fig. 7c, d), which leads to the southward expansion of snow cover extent during those two months (Fig. 5d, f).

The SD experiments reveal that the excessive water equivalent snow depth perturbation in autumn could persist into the ensuing winter, and largely increases snow cover extent in between 40°N and 50°N, especially over the MPV where climatological snow cover is relatively low. The snow cover extent is further enhanced over East China in winter, due to the increased snowfall there. Obviously, the increased snowfall over MPV and East China plays an important role in increasing the surface albedo in situ, and its feedback to local winter circulation could be significant. This will be discussed in the following subsection.

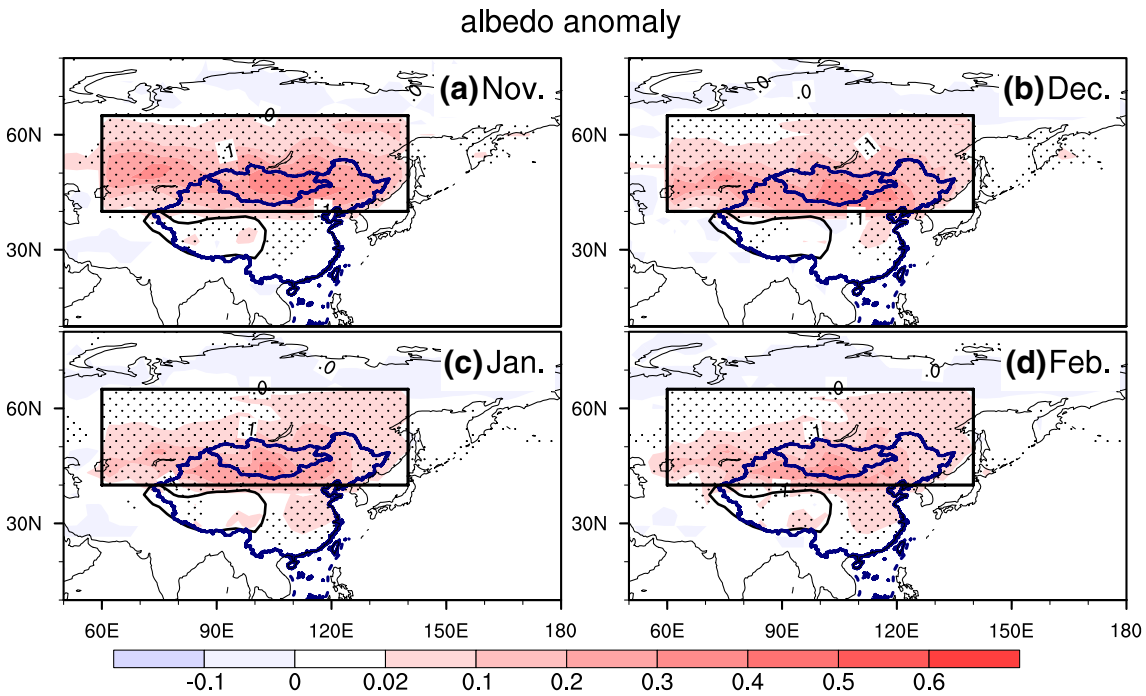

Fig. 6 Composite differences (SD experiment minus control run) of surface albedo in **a** November, **b** December, **c** January, and **d** February from the coupled model experiments. Dots indicate the anomalies of surface albedo significant at the 95% confidence level. The thick black line is the 3000 m height contour, outlining the Tibetan Plateau. The black rectangular denotes the snow mass forcing region

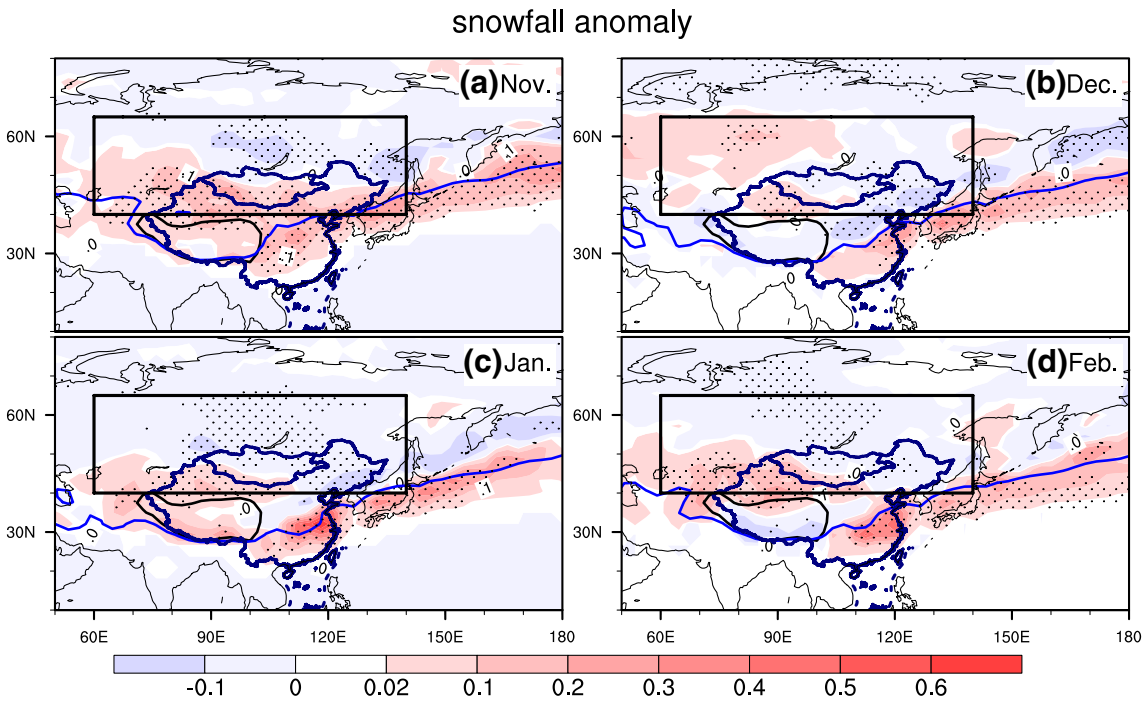

Fig. 7 Same as in Fig. 6 except for the snowfall (mm/day). Blue curves in each panel show the T2m zero contour line. Dots indicate the anomalies of snowfall significant at the 95% confidence level

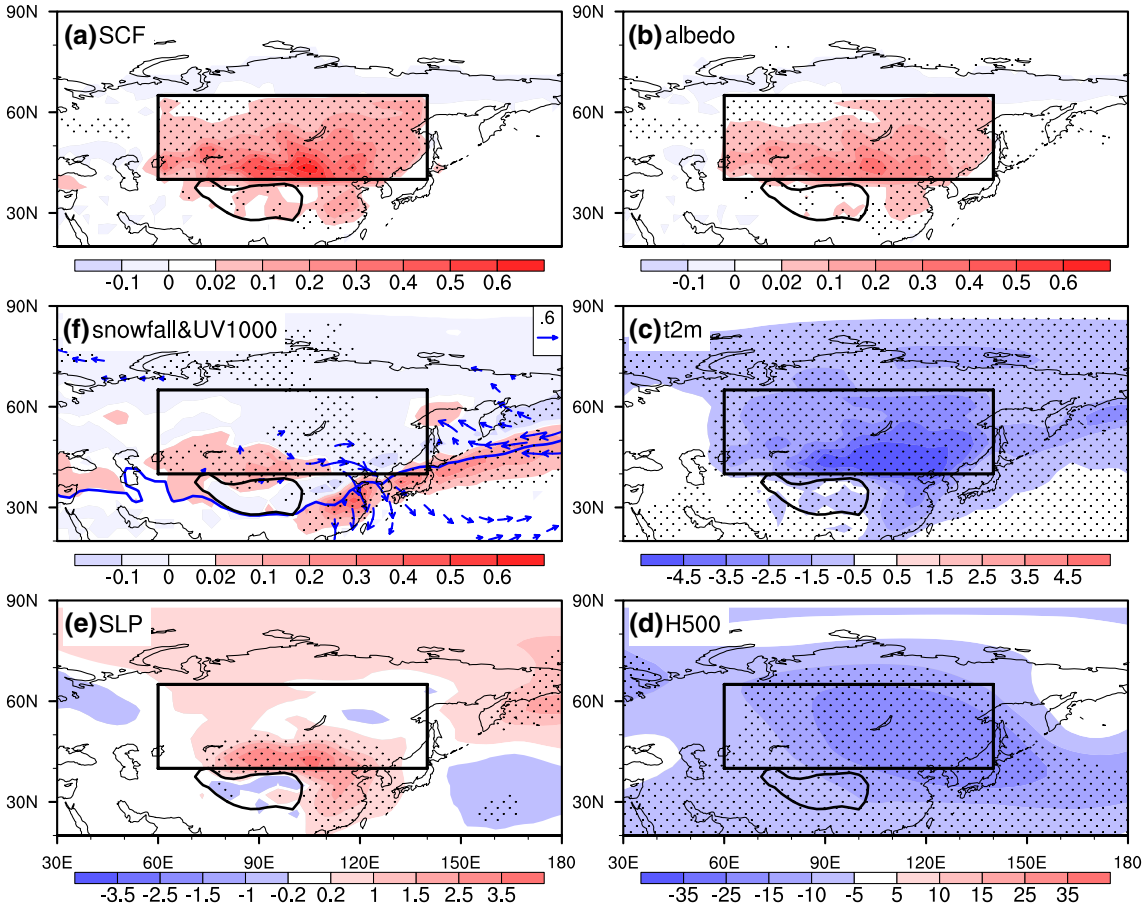

Fig. 8 Winter circulation response to excessive autumn snow depth forcing in the coupled model experiment. Shown are the composite differences between the SD and control experiments in **a** snow cover fraction, **b** surface albedo, **c** 2 m air temperature (T2M), **d** 500 hPa geopotential height (H500), **e** sea level pressure (SLP) and **f** snowfall and 1000 hPa wind anomalies. Dots indicate the scalar anomalies significant at 95% confidence level. Blue curve in **f** denote the T2m zero contour line. The thick black line is 3000 m height contour, outlining the Tibetan Plateau. The black rectangular denotes the region of snow forcing

4.2 Delayed winter circulation anomalies

The winter circulation response to the autumn snow forcing is shown in Fig. 8. The enhanced snow cover extent and surface albedo are located in Mongolian Plateau, the northern China and the central East China (Fig. 8a, b). Figure 8c shows that extensive cooling occurs in the region where surface albedo is largely increased. The maximum cooling reaches −4.5 °C and is located in Mongolia and the northern China. Although Fig. 8c only shows the surface cooling, similar cooling is also observed in 850 and 700 hPa (figure not shown). As a result of the lower-tropospheric cooling, the mid-tropospheric (500 hPa) East Asian trough is enhanced and slightly shifted westward as the climatological trough line is titled from Okhotsk Sea to Yangtze River delta (Fig. 8d). Meanwhile, notable positive sea level pressure anomaly is found over the surface cooling region, which tends to enhance the Mongolian High (Fig. 8e). The anti-cyclonic circulation anomalies associated with the enhanced Mongolian High strengthen northwesterly and northerly winds that induce cold air advection into the central-south East China (Fig. 8f). The circulation anomalies at lower tropospheric levels such as 850 and 700 hPa are relatively weak compared to 500 hPa and SLP (figure not shown). With the southward cold air intrusion, snowfall is enhanced over the East Asia costal region, forming a northeast-southwest titled snowfall band from the Yangtze River Valley to the east of Japan along the EAWM front zone, as well as to the northern flank of TP (Fig. 8f). The increased snowfall over East Asia favors the snow accumulation in winter, and thus caused the locally enhanced snow cover fraction (Fig. 8a) and surface albedo (Fig. 8b). This enhanced snow cover fraction during winter are also detected from observation when the northern part of East Asia experiences a bitter winter (Chen et al. 2014).

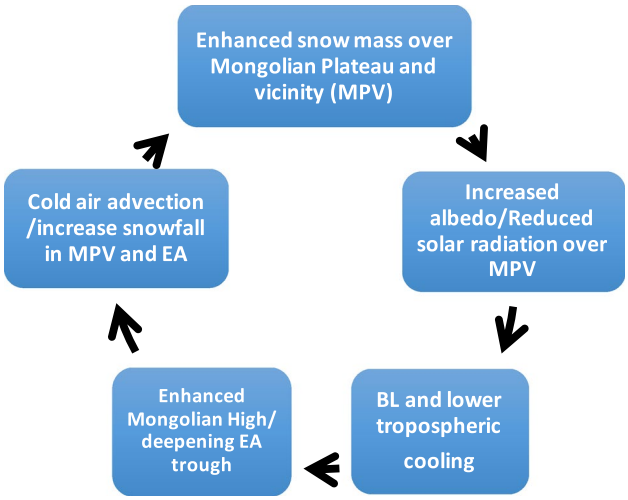

Fig. 9 Schematic diagram showing the positive feedback between Eurasian snow anomalies and the East Asian winter monsoon

4.3 Snow-monsoon feedback process

Based on the above evidence and discussion, we propose a positive snow-EAWM feedback mechanism to characterize the processes by which autumn Eurasian snow depth anomaly affects EAWM climate as illustrated in Fig. 9. The excessive snow depth anomaly persists through the following winter season, and increases surface albedo over mid-latitude Eurasia (40°–50°N), especially the MPV mountain regions. The increased albedo reduces solar radiation received over the surface, leading to coldness in situ and generating a positive SLP anomaly, as well as a negative geopotential height anomaly at 500 hPa. The enhanced Mongolian High and deepened East Asian trough would further enhance southward advection of cold air from the high latitude, increases snowfall over the northern China and the central East China, favoring snow accumulation instead of melting (Fig. 9). The increased snow accumulation in the MPV and East Asia would, in turn, enhance the Mongolian High. Thus, the positive snow-EAWM feedback process maintains snow accumulation anomaly and the anomalous cold air temperature in East Asia. It is also notable that this feedback process extends the anomalous cooling southward, and leads to a large scale of coldness over East Asia.

5 Results from additional sensitivity experiments

5.1 Sensitivity of the winter monsoon anomaly to the location of the autumn snow forcing

To find out whether the persistence of snow depth and snow-EAWM circulation feedback are robust over the entire selected forcing region, we further conducted numerical experiments with prescribing water equivalent snow depth anomalies over three sub-regions, A (40°N–65°N, 40°E–75°E), B (40°N–65°N, 75°E–115°E), C (40°N–65°N, 115°E–140°E), and MPV (40°N–55°N, 80°E–120°E), respectively. The selection of the first three sub-regions follows the results from Luo and Wang (2017), which showed the October snow cover anomalies over different regions have different connections with the EAWM. The MPV is a region where the winter snow cover fraction has the largest variability in the coupled model SD sensitivity experiment.

The results from the coupled model show that the winter monsoon responses to snow mass forcing are generally local, especially the lower boundary temperature anomaly (Fig. 10). The cooling centers are located at the southern edges of the regions A, B, C, and MPV, respectively (Fig. 10

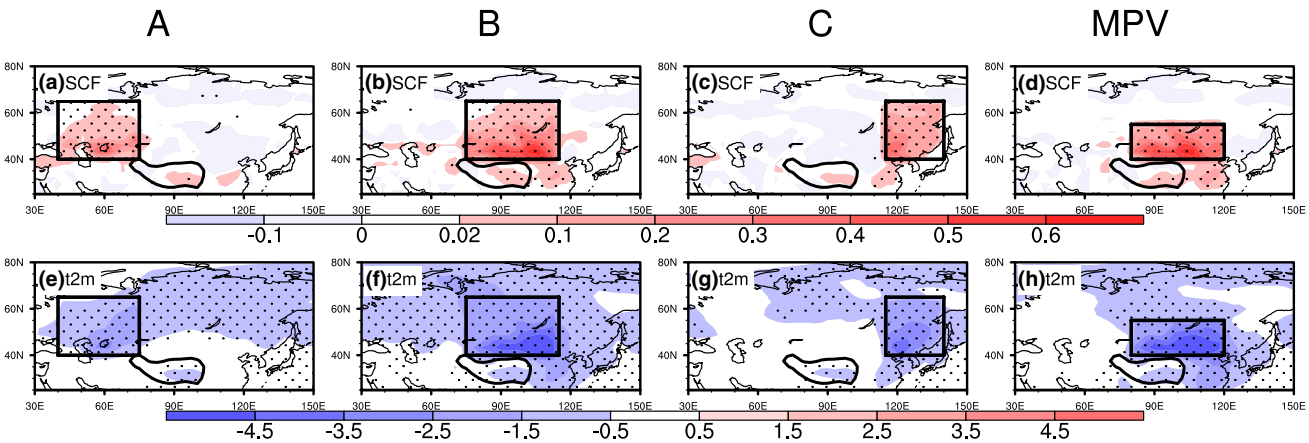

Fig. 10 Composite differences in snow cover fraction anomalies (upper panels) and 2 m temperature anomalies (lower panels) simulated by the coupled model with prescribed excessive snow depth anomalies over key region A, B, C and Mongolian Plateau vicinity (MPV), respectively

lower panels). The snow mass anomaly in region B may have a substantial impact on East Asian winter climate as it can induce a broad range of cooling over East Asia. The enhanced snow mass in region C can induce cold winter over the northeast China. More importantly, based on the model results, the MPV region turns out to be a key region where the excessive autumn snow mass could lead to wintertime coldness over East Asia (Fig. 11d, f). The MPV domain is generally consistent with the region B, except eliminating the area to the north of 55°N.

5.2 Possible role of atmosphere–ocean coupling

Comparison of the coupled model and AGCM alone experiment results can help to identify the role of the atmosphere–ocean coupling. The winter circulation anomalies associated with autumn anomalous snow depth forcing derived from the atmospheric component of the coupled model, the ECHAM5.3, are shown in Fig. 11. The anomaly patterns are generally consistent with those from the coupled model. However, the intensities of the anomalous circulations are weaker compared with those derived from the coupled model, i.e., the cooling center over East Asia reaches − 3.5 °C and pressure anomalies center is around 2.5 hPa at SLP (Fig. 11c, e). The mild influences on winter circulation simulated by ECHAM model are corresponding to the weaker snow depth accumulation in ECHAM model (figure not shown). Due to atmosphere–ocean interaction (AOI), the East Asian trough shifts southward, deepening over Japan (figure not shown). The deepened 500 hPa trough and the increased land–ocean pressure gradients over East Asia enhance northwesterly winds, which decrease the temperature, meanwhile increase the snowfall along the EAWM front zone, thereby amplifying the snow-EAWM feedback.

5.3 Results from specified albedo experiment

Results from SD experiments have suggested a positive snow-EAWM feedback could lead to intensified EAWM. Snow mass is proved to be a key parameter because it can persist into winter and is also actively involved in this feedback process. However, apart from snow mass, it is also necessary to address whether albedo variations, as another

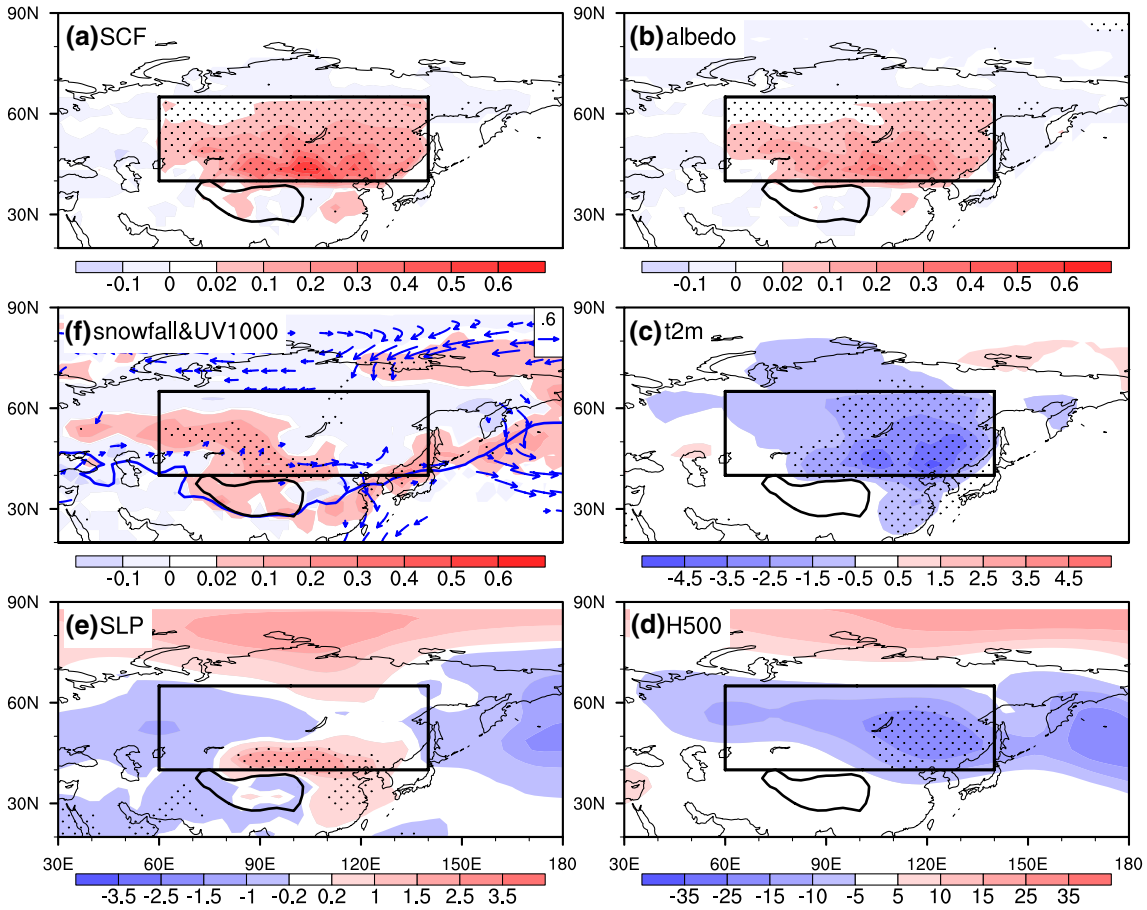

Fig. 11 Same as in Fig. 8 except for the results in the ECHAM model experiments

key link in the feedback process, can persist from autumn to winter and influence wintertime circulation anomalies.

To examine this issue, we first perform a paired albedo experiments to evaluate the impact of the autumn albedo anomaly on the ensuing winter circulation. In the first set of experiments, the albedo over the central Eurasian region is multiplied by a factor of 1.2 in October and November, which is named as enhanced albedo experiment (+ AL2). The second set of experiments resembles the first set, except that the factor is replaced with 0.8, and is denoted as reduced albedo experiment (− AL2). The difference between (+ AL2) and (− AL2) is regarded as the atmospheric response. It turns out the difference in surface albedo between (+ AL2) and (− AL2) disappears immediately in December, and correspondingly no significant wintertime circulation anomalies can be found (figures not shown).

A second paired experiments similar to (+ AL2, − AL2) are performed, except that albedo modification is prolonged into midwinter, i.e., from October 1 to January 31, and they are named as (+ AL4) and (− AL4), respectively. Results from (+ AL4) and (− AL4) experiments show significant wintertime circulation anomalies (Fig. 12). The anomalous low at 500 hPa deepens the East Asian trough, meanwhile, the positive SLP anomalies at mid-latitude East Asia enhance the Mongolian High, and notable surface cooling is also observed at mid-high latitude Eurasian continent (Fig. 12). The positive anomalous SLP over mid-latitude Eurasia in Fig. 12c has a similar location as the that in the SD experiments in Fig. 8e, Meanwhile, the composite difference between (+ AL4) and (− AL4) again show enhanced snowfall at East Asia (figure not shown), which implies it also involves a snow-EAWM circulation feedback process (Fig. 9) as we found in SD experiment. Note that the albedo experiment verifies that the surface albedo acts as an important link in the feedback loop in influencing the EAWM. The results from ECHAM model experiment are again similar to what we found in the coupled model, but with less intensity.

6 Summary and discussion

We have shown that the leading mode of interannual variability of the mean snow cover extent in October and November is characterized by a continental scale of excessive (or suppressed) snow cover anomaly covering the domain of 40°N–65°N, 60°E–140°E. This central Eurasian domain is therefore selected as the forcing region for our numerical experiments.

Using a coupled model NUIST-ESM, we perform a control run and SD sensitivity experiments to identify how the autumn snow mass impacts the subsequent winter climate. The SD experiment is designed with prescribed positive snow depth anomaly over the Eurasian forcing domain in

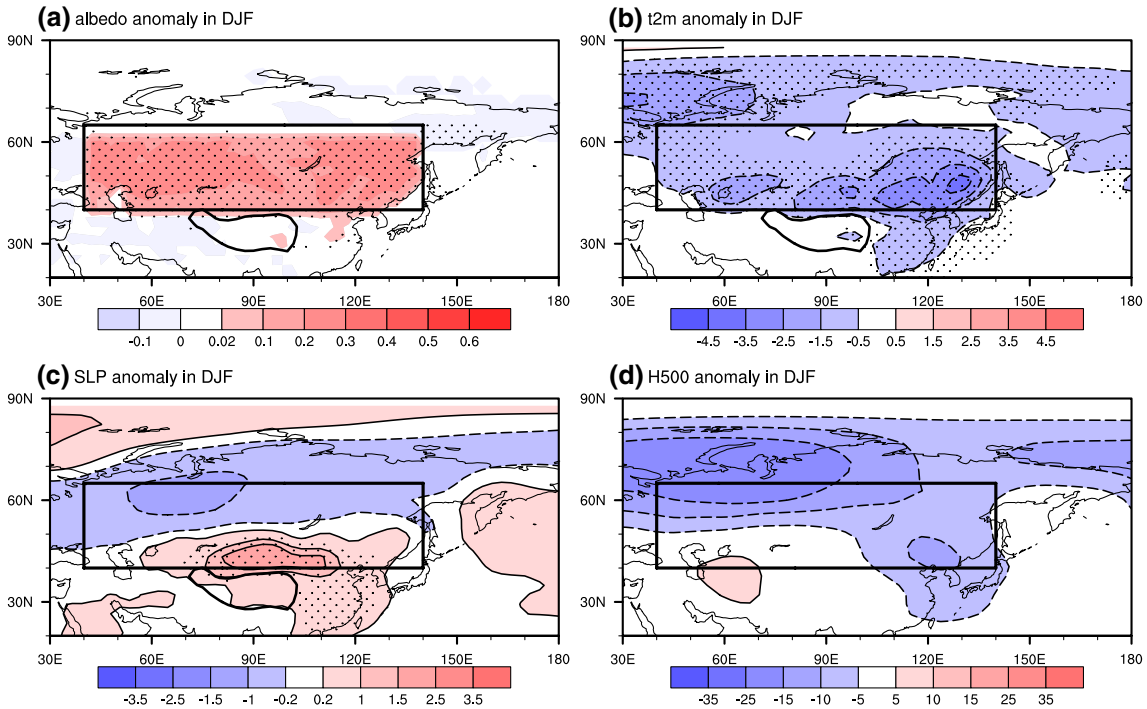

Fig. 12 Winter circulation response in the albedo forcing experiment. Composite differences of **a** albedo, **b** 2 m air temperature (T2M), **c** sea level pressure (SLP), **d** 500 hPa geopotential height (H500) between (+ AL4) and (− AL4) in the coupled model experiments

October and November, and after December 1 the model runs without snow depth perturbation.

6.1 Summary

The model results show that an excessive snow mass in autumn can enhance the subsequent EAWM and increase winter snowfall over mid-latitude East Asia, i.e., the northwestern China and along the EAWM front zone stretching from the southeast China to Japan.

The physical processes by which an autumn snow anomaly affect EAWM involves a positive snow-EAWM feedback mechanism. The excessive autumn snow depth anomaly can persist throughout the following winter season, significantly enhancing the snow cover extent in the mid-latitude Eurasia between 40°N and 50°N, especially over the Mongolian Plateau and vicinity (MPV) region. The increased surface albedo over Eurasia and reduced solar radiation received at the surface cool lower-troposphere in situ, which enhances the Mongolian High and deepens East Asian trough. The later, further reinforce southward advection of cold air from the high latitude. Cold air advection causes the snow accumulation over the MPV and the southeastward extension of snow cover to the southeast China, which will feedback to enhance EAWM system through changing albedo.

Model results suggest that the MPV is a key region where excessive autumn snow mass could induce substantial coldness in the following winter over East Asia. The results also show that the snow mass accumulation over the northern central Eurasia between 50°–65°N does not have significant influences on the winter monsoon south of 45°N. The wintertime circulation responses, especially the surface air temperature response, to autumn snow anomalies are generally local.

We also find that the coupled model reproduces similar winter anomalous circulation patterns as the AGCM experiments but the magnitude of the anomaly is larger. This is related to a more efficient accumulation of the prescribed excessive snow depth anomaly in the coupled model simulation.

The results from AL2 experiments suggest that surface albedo does not have a "memory" effect. When the added albedo anomaly is switched off on December 1, its impact on atmospheric circulation terminates immediately and could not persist into winter. Only when the specified albedo anomalies are artificially prolonged into December and January, the snow-EAWM feedback process could be stimulated.

6.2 Discussion

The feedback process between the snow depth and winter circulation anomalies reproduced in the coupled model provides a robust physical basis for the delayed influence of autumn snow on winter climate. Thus, snow mass anomaly is confirmed as a source of predictability in seasonal prediction.

Some previous studies have proposed that an increase in snow cover over Siberia could yield a negative AO anomaly (Gong et al. 2003; Cohen et al. 2007) through a process involving vertical wave propagation from troposphere to stratosphere. In the present study, we did not find AO-related circulation anomalies in the SD experiments. This may be because ECHAM 5.3 model only has 31 vertical levels, which is incapable of capturing the vertical propagating waves and the stratosphere-troposphere interaction.

We found both persistence process of snow mass anomaly in winter (Fig. 3) and the snow-EAWM feedback process could lead to accumulation of snow mass and increase Eurasian snow cover fraction in winter. An interesting question is which process of the above two is more important? The time series of water equivalent snow depth averaged over the MPV from the coupled model show that the snow depth in the sensitivity SD run accumulates at the same rate as in the control run (figure not shown), which suggests the snow mass accumulation is the major process that caused excessive snow anomaly over the MPV in winter. However, over the southern EA (30°N–40°N, 105°E–120°E) the snow-monsoon feedback process is essential as evidenced by the excessive snowfall along the EAWM front zone (Fig. 8f).

The sensitivity tests suggest that the degree of snow mass's impacts on winter monsoon is positively related to the extent of the specified autumn water equivalent snow depth. In our experiment, an 8 cm/month of water equivalent snow depth was specified as an initial perturbation, which may exaggerate the observed snow depth anomaly. However, sensitivity experiments with 6 or 4 cm/month snow depth anomaly that are specified in the preceding autumn produced similar anomalous circulation patterns as those in the 8 cm/month water equivalent snow depth experiment except with reduced intensity. Observational analysis suggests the enhanced snow cover fraction during winter can be observed when the northern part of East Asia experiences a bitter winter, and this supports part of the snow-EAWM feedback process. However, more observational analysis should be further conducted.

Acknowledgements This work is supported by the National Science Foundation (Climate Dynamics Division) Award No. AGS-1540783 and the NOAA/CVP #NA15OAR4310177, as well as the National Natural Science Foundation of China (Grant No. 41420104002) and the National Key Research and Development Program of China (Grant No. 2016YFA0600401). This is publication No. 10292 of the SOEST, publication No. 1302 of IPRC, and publication No. 200 of Earth System Modeling Center (ESMC).

References

Barnett TP, Dümenil L, Schlese U, Roeckner E, Latif M (1989) The effect of Eurasian snow cover on regional and global climate variations. J Atmos Sci 46:661–686. https://doi.org/10.1175/1520-0469(1989)046<0661:teoesc>2.0.co;2

Cao J et al (2015) Major modes of short-term climate variability in the newly developed NUIST Earth System Model (NESM). Adv Atmos Sci 32:585–600. https://doi.org/10.1007/s00376-014-4200-6

Chen Z, Wu R, Chen W (2014) Distinguishing interannual variations of the northern and southern modes of the East Asian winter monsoon. J Clim 27:835–851. https://doi.org/10.1175/jcli-d-13-00314.1

Clark MP, Serreze MC (2000) Effects of variations in East Asian snow cover on modulating atmospheric circulation over the North Pacific Ocean. J Clim 13:3700–3710. https://doi.org/10.1175/1520-0442(2000)013<3700:EOVIEA>2.0.CO;2

Cohen J, Entekhabi D (1999) Eurasian snow cover variability and northern hemisphere climate predictability. Geophys Res Lett 26:345–348. https://doi.org/10.1029/1998GL900321

Cohen J, Fletcher C (2007) Improved skill of northern hemisphere winter surface temperature predictions based on land–atmosphere fall anomalies. J Clim 20:4118–4132. https://doi.org/10.1175/jcli4241.1

Cohen J, Barlow M, Kushner PJ, Saito K (2007) Stratosphere–troposphere coupling and links with Eurasian land surface variability. J Clim 20:5335–5343. https://doi.org/10.1175/2007jcli1725.1

Fletcher CG, Hardiman SC, Kushner PJ, Cohen J (2009) The dynamical response to snow cover perturbations in a large ensemble of atmospheric GCM integrations. J Clim 22:1208–1222. https://doi.org/10.1175/2008jcli2505.1

Furtado JC, Cohen JL, Butler AH, Riddle EE, Kumar A (2015) Eurasian snow cover variability and links to winter climate in the CMIP5 models. Clim Dyn 45:2591–2605. https://doi.org/10.1007/s00382-015-2494-4

Gong G, Entekhabi D, Cohen J (2003) Modeled northern hemisphere winter climate response to realistic siberian snow anomalies. J Clim 16:3917–3931. https://doi.org/10.1175/1520-0442(2003)016<3917:mnhwcr>2.0.co;2

Hahn DG, Shukla J (1976) An apparent relationship between Eurasian snow cover and Indian monsoon rainfall. J Atmos Sci 33:2461–2462. https://doi.org/10.1175/1520-0469(1976)033<2461:aarbes>2.0.co;2

Hardiman SC, Kushner PJ, Cohen J (2008) Investigating the ability of general circulation models to capture the effects of Eurasian snow cover on winter climate. J Geophys Res Atmos. https://doi.org/10.1029/2008JD010623

Honda M, Inoue J, Yamane S (2009) Influence of low Arctic sea-ice minima on anomalously cold Eurasian winters. Geophys Res Lett. https://doi.org/10.1029/2008GL037079

Jhun J-G, Lee E-J (2004) A new East Asian winter monsoon index and associated characteristics of the winter monsoon. J Clim 17:711–726. https://doi.org/10.1175/1520-0442(2004)017<0711:ANEAWM>2.0.CO;2

Li J, Wang B, Yang Y-M (2016) Retrospective seasonal prediction of summer monsoon rainfall over West Central and Peninsular India in the past 142 years. Clim Dyn 48:2581–2596. https://doi.org/10.1007/s00382-016-3225-1

Luo X, Wang B (2017) Predictability and prediction of the total number of winter extremely cold days over China. Clim Dyn. https://doi.org/10.1007/s00382-017-3720-z

North GR, Bell TL, Cahalan RF, Moeng FJ (1982) Sampling errors in the estimation of empirical orthogonal functions. Mon Weather Rev 110:699–706

Peings Y, Saint-Martin D, Douville H (2012) A numerical sensitivity study of the influence of siberian snow on the northern annular mode. J Clim 25:592–607. https://doi.org/10.1175/jcli-d-11-00038.1

Robinson DA, Dewey KF, Heim RR Jr (1993) Global snow cover monitoring: an update. Bull Am Meteorol Soc 74:1689–1696. https://doi.org/10.1175/1520-0477(1993)074<1689:gscmau>2.0.co;2

Robinson DA, Estilow TW, NOAA-CDR-Program (2012) NOAA Climate Date Record (CDR) of northern hemisphere (NH) snow cover extent (SCE), version 1. [indicate subset used]. NOAA Natl Clim Data Cent. https://doi.org/10.7289/V5N014G9 (access date)

Roeckner E et al (2003) The atmospheric general circulation model ECHAM 5. Part I: model description. MPI Report 349, Max Planck Institute for Meteorology, Hamburg, p 127

Roesch A, Roeckner E (2006) Assessment of snow cover and surface albedo in the ECHAM5 general circulation model. J Clim 19:3828–3843. https://doi.org/10.1175/jcli3825.1

Wang L, Chen W (2013) The East Asian winter monsoon: re-amplification in the mid-2000s Chinese. Sci Bull 59:430–436. https://doi.org/10.1007/s11434-013-0029-0

Wang L, Lu M-M (2016) The East Asian winter monsoon. The global monsoon system: research and forecast, vol 5, 3rd edn. World Scientific, Singapore

Wang B, Wu R, Fu X (2000) Pacific-East Asian teleconnection: how does ENSO affect East Asian climate? J Clim 13:1517–1536

Wang L, Huang R, Gu L, Chen W, Kang L (2009) Interdecadal variations of the East Asian winter monsoon and their association with quasi-stationary planetary wave activity. J Clim 22:4860–4872. https://doi.org/10.1175/2009JCLI2973.1

Wang B, Wu Z, Chang C-P, Liu J, Li J, Zhou T (2010) Another look at interannual-to-interdecadal variations of the East Asian winter monsoon: the northern and southern temperature modes. J Clim 23:1495–1512. https://doi.org/10.1175/2009jcli3243.1

Watanabe M, Nitta T (1998a) Decadal changes in the atmospheric circulation and associated surface climate variations in the northern hemisphere winter. J Clim 12:494–510. https://doi.org/10.1175/1520-0442(1999)012<0494:DCITAC>2.0.CO;2

Watanabe M, Nitta T (1998b) Relative impacts of snow and sea surface temperature anomalies on an extreme phase in the winter atmospheric circulation. J Clim 11:2837–2857. https://doi.org/10.1175/1520-0442(1998)011<2837:RIOSAS>2.0.CO;2

Wu B, Su JZ, Zhang R-H (2011) Effects of autumn–winter Arctic sea ice on winter Siberian High. Chin Sci Bull 56:3320. https://doi.org/10.1007/s11434-011-4696-4

Yim S-Y, Jhun J-G, Lu R, Wang B (2010) Two distinct patterns of spring Eurasian snow cover anomaly and their impacts on the East Asian summer monsoon. J Geophys Res Atmos. https://doi.org/10.1029/2010JD013996

Zhang R, Sumi A, Kimoto M (1996) Impact of El Niño on the East Asian monsoon. J Meteorol Soc Jpn Ser II 74:49–62